RSC Advances

ROYAL SOCIETY OF CHEMISTRY

www.rsc.org/advances

Journal Name

ARTICLE

Conformational behaviour of 3-methyl-4-(4-methylbenzoyl)-1-phenyl-pyrazol-5-one: a sudden story of three desmotrops†

0Received 00th January 20xx,
Accepted 00th January 20xx

DOI: 10.1039/x0xx00000x

www.rsc.org/

Vanya B. Kurteva,[a,*] Boris L. Shivachev,[b] Rositsa P. Nikolova,[b] Svetlana D. Simova,[a] Liudmil M. Antonov,[a] Lubomir A. Lubenov,[a] Maria A. Petrova[c]

The conformational behavior of 3-methyl-4-(4-methylbenzoyl)-1-phenyl-pyrazol-5-one was studied using a combination of X-ray diffraction, NMR spectroscopy in solution and solid state, and DFT calculations in gas phase. The compound can adopt four different tautomers, determined by the combination of the keto-enol tautomerism of pyrazolone and the attached 4-acyl carbonyl group. Potential energy surfaces simulations in gas phase show that each of the tautomeric forms has stable conformers, defined by energy minima, which could potentially be obtained in solid state. The NMR analyses indicate that the keto-enol conformations with intramolecular H-bonding are preferred in solutions. Crystallization trials produced five different crystal phases; three yellow and two colorless. The single crystal XRD and solid state NMR structural analyses revealed that three desmotrops are obtained, two of them as two different conformational polymorphs. The difference in the coloration is attributed to the displacement of the double bound producing different conjugation of the pyrazolone. Studies on the effect of solvent on the solid state structure could not produce a systematic trend and in fact the most part of the studied crystal phases could be obtained from acetone solution. The investigations on the factors governing the crystalization of different phases, temperature, concentration and solvent nature, are in progress.

Introduction

The ability of a given compound to crystallize in more than one polymorph modification is among the most studied areas of modern solid state chemistry.[1] Due to the different packing and/or molecular conformation the polymorph modifications differ in their physical and chemical properties, such as stability, solubility, density, melting point, dissolution rate, morphology, colour etc. This behaviour can have a profound impact in the drug design, because such variations of solid state properties desired or not, may influence every stage of the product development.[2] The special case of polymorphism, closely related with tautomerism, is termed desmotropy. Based on numerous publications and definitions, summarized by Elguero,[3] it can be stated that if a compound can crystallize in more than one stable tautomeric form, it possess desmotropism. To the best of our knowledge, there are no examples in the literature on the isolation of more than two desmotrops of a given molecule.

Pyrazolones constitute an important class of heterocyclic compounds due to the diverse pharmacological activity profiles displayed; antibacterial, antifungal, antioxidant, antitumor, antihelmintic, anti-inflammatory, analgesic, antipyretic, antiischemic, antianxiolytic, etc. 4-Acylpyrazol-5-ones are among the most widely exploited O-donors in coordination chemistry.[4] First studied by Jensen,[5] the chelating behaviour of this class of β-dicarbonyl compounds has received immense attention due to several valuable properties of their complexes, such as vast extracting ability, great separation power and intense colour. Acylpyrazolones are known from the end of 19th century,[6] but the advantageous fast and efficient synthetic protocol developed in 1959 by Jensen,[7] practically has no concurrence and is intensively exploited till nowadays. However, the question about the conformational preferences, which is related to the complexation properties, is still controversial and considerable efforts are directed towards its clarification. The studied compound 1-phenyl-3-methyl-4-(4-methylbenzoyl)-pyrazol-5-one contains a pyrazole ring fused to a chelating arm and can adopt four different tautomers, defined by the keto-enol tautomerism of pyrazolone unit and the attached 4-acyl carbonyl group. These tautomeric forms are presented on Scheme 1 (**A**, **B**, **C**, **D**). Additionally, each tautomer can have a number of different rotamers depending on the rotation around three bonds: C(pyrazol)-C, C-Ar or N(pyrazole)-C(Ph) bond.

[a] *Institute of Organic Chemistry with Centre of Phytochemistry, Bulgarian Academy of Sciences, Acad. G. Bonchev str., bl. 9, 1113 Sofia, Bulgaria.*
[b] *Institute of Mineralogy and Crystallography "Acad. Ivan Kostov", Bulgarian Academy of Sciences, Acad. G. Bonchev str., bl. 107, 1113 Sofia, Bulgaria.*
[c] *University of Chemical Technology and Metallurgy, Department of General and Inorganic Chemistry, 8 Kliment Ohridski blvd., 1756 Sofia, Bulgaria.*
† Dedicated to our colleague and friend Prof. DSc Ivan Pojarlieff on the occasion of his 80th anniversary.
Electronic Supplementary Information (ESI) available: [details of any supplementary information available should be included here]. See DOI: 10.1039/x0xx00000x

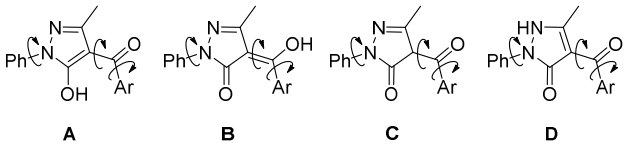

Scheme 1. Sketch of the possible tautomers of 4-aroyl-3-methyl-1-phenyl-pyrazol-5-ones.

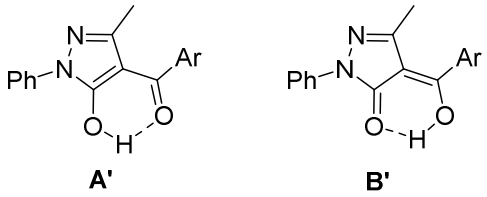

Scheme 2 Stabilization of the enol molecular structure by intramolecular hydrogen O-H…O bond and thus obstructing of the rotation around C(pyrazol)-C bond.

Intramolecular hydrogen bonding O-H…O (Scheme 2) can additionally stabilize structures **A** and **B**, if the oxygen's are adjacent to each. If such hydrogen bonding is realized, additional energy for disrupting it will be required for rotation around the C4-C-aroyl bond.

Thus one could assume that in such case the variety of rotamers for **A** and **B** would be a function of the rotation of the Ar or Ph substituents only (Scheme 2).

Michaelis and Engelhardt[8] have reported the isolation of keto and enol forms of 1-phenyl-3-methyl-4-benzoyl-pyrazol-5-one. Later, Jensen[5] specified that the keto-tautomers could be obtained by recrystallization from polar solvents as colourless crystals, while the enol-tautomers crystalize from non-polar solvents as yellowish crystals. Holzer *et al.*[9] have fixed two individual tautomers of a series of acylpyrazolones by Mutsunobu alkylation and have determined their structures by NMR and X-ray studies.[10] The authors have found that the conformational preferences are strongly dependent on the solvent and observed that during melting keto-form changed into enol one. The desmotropy of 4-acylpyrazolones has been also studied by solid state ^{15}N NMR by Holzer *et al.*[11]. It has found that benzoyl pyrazolone exhibits desmotropy and crystals of two tautomers were obtained from different solvents. Contrary to 4-benzoyl and 4-thiophenoyl products, substituted benzoyl derivatives are poorly studied. To the best of our knowledge, only Reddy *et al.*[12] report on the isolation and single crystal structure determination of 4-methylbenzoyl pyrazolone; the solvent not indicated.

Herein, we report on the conformational behaviour of 3-methyl-4-(4-methylbenzoyl)-1-phenyl-pyrazol-5-one studied by X-ray diffraction in solid state, NMR spectroscopy in solution and in solid state, and DFT calculations in gas phase. Despite the motivation for this work was accidental, as will be clarified bellow, it led to isolation of five different crystal phases of the title compound and excellent agreement between experimental and theoretical data.

Results and discussion

The title compound, 3-methyl-4-(4-methylbenzoyl)-1-phenyl-pyrazol-5-one,[13] was obtained according to an adapted literature procedure[7] in excellent yield.[14] Surprisingly, the product's melting point was more than 20°C higher than the literature one.[15] The latter provoked numerous crystallization experiments.

Several solvent systems were used in order to obtain single crystals suitable for X-ray structural analyses. The emphasis was given on the most widely used in metal ion extractions (hydrocarbons and halogenated hydrocarbons) and solid state complex formations (alcohols, alcohol-acetone or alcohol water) solvents and solvent systems. All crystal phases were grown from clear solutions in closed vessels at room temperature. Five types of crystals were isolated (Figure S1): fine yellow needles from heptane, chloroform, or acetonitrile with m. p. 101.1-101.2°C (**1**); two polymorphs from ethanol/water – thick pale yellow needles with m. p. 103.9-104.0°C (**2**) and yellow needles with m. p. 105.8-105.9°C (**3**); thick colourless plates from methanol/acetone with m. p. 126.2-126.4°C (**4**); and colourless needles from methanol/water with 135.4-135.6°C (**5**). The purity of the crystal phases was assessed by powder X-Ray diffraction (Figure S2). Polymorphs **1**, **4** and **5** were grown as single phases, while **2** and **3** were obtained as a mixture of phases. Crystals of **2** and **3** for single crystal XRD and m. p. determination were collected under a microscope.

Several unexpected features of the crystallizing process were observed.

1. All crystal phases were grown from yellow solutions.
2. Almost all crystal phases could be grown from acetone and from ethanol-water by varying the dilution and temperature; gentle heating below boiling point *vs* refluxing.
3. Four different types of crystals were obtained from ethanol/water solutions. Colourless needles (**5**) with m. p. 126.2-126.4°C were grown under heating at ca. 50°C, conditions similar to methanol/water system, independently on the concentration and water content, while two yellow crystals (**2** and **3**) were isolated under reflux as a mixture of phases and the third yellow polymorph **1** as a single phase or as a mixture with **2**.

The combination of facts that (i) the initial solution is always yellow coloured and (ii) one can obtain colourless crystals suggests that in solution (at least for the employed solvents or solvent systems) various tautomers are present simultaneously. As we could not achieve a colourless solution, even after dissolving colourless crystal forms, one can hypothesizes that the yellow, e.g. enol forms with OH and =O present, are predominated over the keto ones.

Crystal samples of **1**, **2**, **3**, **4** and **5** were investigated by X-Ray single crystal analyses. The data were collected at both room (RT, 290K) and low temperature (LT, 150 K) in order to locate more precisely the positions of hydrogen atoms and to study the possibilities for temperature dependent switching between different tautomeric forms. Details of data collection

Table 1 Crystal data and the structure refinement indicators for the studied phases.

	1	**2**	**3**	**4**	**5**
Crystal system	Monoclinic	Monoclinic	Orthorhombic	Monoclinic	Monoclinic
Space group	$P2_1/n$	$P2_1/c$	$Pna2_1$	$P2_1/c$	C2/c
T(K)	290	290	290	290	290
Radiation, wavelength (Å)	Mo K*a*, 0.71073	Mo K*a*, 0.71073	Mo K*a*, 0.71073	Mo K*a*, 0.71073	Mo K*a*, 0.71073
a (Å)	15.3847(5)	11.8744(7)	7.6533(5)	10.966(5)	29.438(1)
b (Å)	5.2035(2)	5.3140(5)	17.3165(8)	12.084(5)	9.049(1)
c (Å)	18.2280(7)	23.4934(14)	11.3945(5)	11.968(5)	11.4945(1)
V(Å^3)	1459.04(10)	1471.17(19)	1510.09(14)	1488.9(11)	3036.3(2)
α (°)	90	90	90	90	90
β (°)	90.913(3)	97.072(5)	90	110.14(4)	97.46(1)
γ (°)	90	90	90	90	90
Z	4	4	4	4	8
F_{000}	616	616	616	616	1232
d (mg. m^{-3})	1.331	1.32	1.309	1.304	1.279
μ (mm^{-1})	0.088	0.087	0.087	0.086	0.085
Cell parameters	from 6513 refl.	from 2230 refl.	from 1744 refl.	from 4123 refl.	from 2842 refl.
Crystal habit, color	prism, yellow	prism, yellow	prism, yellow	prism, colourless	prism, colourless
Crystal size (mm^3)	0.28× 0.22× 0.20	0.20 ×0.19 × 0.16	0.25 ×0.22 × 0.19	0.4 × 0.4 × 0.35	0.40 × 0.13 × 0.11
R1 ($F^2 > 2\sigma(F^2)$)	0.052	0.0566	0.0706	0.043	0.053
wR2 (all data)	0.142	0.1544	0.191	0.118	0.148
$\Delta\rho_{max}$/ $\Delta\rho_{min}$ (e Å^{-3})	0.18/-0.18	0.037/-0.186	0.052/-0.229	0.16/-0.17	0.24/-0.18
Crystal system	Monoclinic	Monoclinic	Orthorhombic	Monoclinic	Monoclinic
Space group	$P2_1/n$	$P2_1/c$	$Pna2_1$	$P2_1/c$	C2/c
T(K)	150	150	150	150	150
Radiation, wavelength (Å)	Mo K*a*, 0.71073	Mo K*a*, 0.71073	Mo K*a*, 0.71073	Mo K*a*, 0.71073	Mo K*a*, 0.71073
a (Å)	15.3324(6)	11.7774(7)	7.4723(5)	11.8263(3)	29.429(1)
b (Å)	5.1202(2)	5.315(1)	17.3131(8)	12.084(5)	8.8477(5)
c (Å)	18.0418(7)	23.349(3)	11.3273(5)	11.9472(4)	11.4839(6)
V(Å^3)	1416.16(10)	1449.0(5)	1465.40(14)	1453.49(9)	2964.8(3)
α (°)	90	90	90	90	90
β (°)	90.979(4)	97.592(7)	90	110.334(4)	97.468(5)
γ (°)	90	90	90	90	90
Z	4	4	4	4	8
F_{000}	616	616	616	616	1232
d (mg. m^{-3})	1.371	1.34	1.286	1.304	1.279
μ (mm^{-1})	0.091	0.088	0.088	0.088	0.087
Cell parameters	from 3100 refl.	from 2230 refl.	from 844 refl.	from 5644 refl.	from 3054 refl.
Crystal habit, color	prism, yellow	prism, yellow	prism, yellow	prism, colourless	prism, colourless
Crystal size (mm^3)	0.28× 0.22× 0.20	0.20 ×0.19 × 0.16	0.25 ×0.22 × 0.19	0.4 × 0.4 × 0.35	0.40 × 0.13 × 0.11
R1 ($F^2 > 2\sigma(F^2)$)	0.038	0.0496	0.070	0.04	0.044
wR2 (all data)	0.104	0.119	0.200	0.111	0.136
$\Delta\rho_{max}$/ $\Delta\rho_{min}$ (e Å^{-3})	0.21/-0.27	0.237/-0.237	0.214/-0.308	0.23/-0.316	0.242/-0.252

procedure, corresponding structural data and refinement indicators are presented in Table 1.

The atomic positions of non-hydrogen atoms in the studied structures were located from the electron density maps for both RT and LT experiments. It was found that in each of the studied crystal structures there is only one molecule in the asymmetric unit which indicates that individual crystal samples represent only one tautomeric form of the studied molecule (Figure 1).

The C5-O5 and C41-O41 distances (Table S1) indicate clearly that structures **1** and **2** are built of tautomer **A'** independently on the temperature of the data collection, the LT structure of **3** is also built by **A'** form tautomer, the RT structure of **3** is a mix of **A'** and **B'** tautomers, while structures **4** and **5** present packing of tautomer **D** irrespective of the temperature (Schemes 1 and 2).

The hydrogen atoms of the aromatic rings and methyl groups for all of the studied structures were included on calculated positions. All of the hydrogen atoms were allowed to ride on the neighbouring atoms with relative isotropic displacement coefficients. In order to determine individual tautomers in structures **1**, **2** and **3** the hydroxyl hydrogen atom had to be localized. On the difference Fourier maps for LT experiments the hydroxyl hydrogen atom was clearly visible to be next to O5 atom for all three structures. In addition the truthful positioning of the H (O41 or O5) atom was performed with respect to observed C5-O5 and C41-O41 distances. The C5-O5 and C41-O41 distances, based on LT data, are respectively 1.310(1) and 1.262(1) Å in structure **1**; 1.323(3) 1.259(3) in structure **2**; 1.325(7) and 1.290(7) Å in structure **3**. The corresponding distances obtained from the RT and LT data show similar values for structures **1** and **2**, 1.303(2), 1.272(2) Å and 1.311(3), 1.268(3) Å respectively, while for structure **3** the C5-O5 and C41-O41 distances are almost equal with values of 1.301(6) and 1.289(7) Å; the difference is in range of the error. The latest finding suggests that the proton in structure **3** at RT

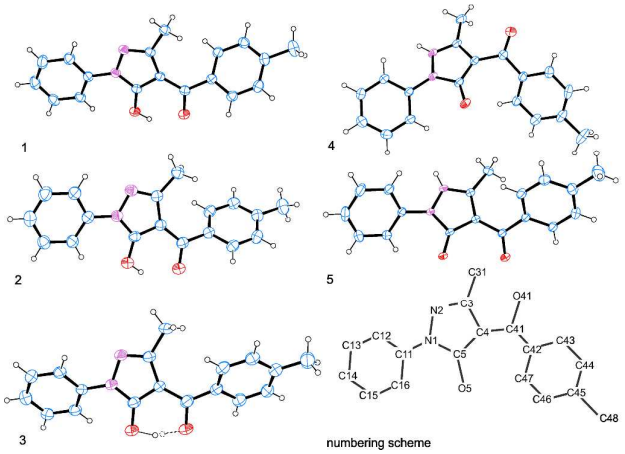

Figure 1 ORTEP drawing of the isolated polymorphs 1-5 and atom labelling scheme; the hydrogen atoms are shown as small sphere of arbitrary radii. The proton in structure **3** is connected with thick line with O5 and with dotted line with O41 to represent both RT and LT diffractions.

is equally distanced from O5 and O41 atoms. Actually the highest electron density on the difference Fourier map in this case is 1.13 Å distant from O41 atom and at 1.35 Å from O5 (Table S1, Figure S3). Although the RT experimental data should not be a prerequisite for making conclusions on the positions of hydrogen atoms, the aforementioned distances indicate that the structure of **3** at RT presents packing of **B'** tautomer and that the difference between the energy minima of **A'** and **B'** tautomers is insignificant as it is indicated by the results of the DFT calculation (see below). Understandably, at RT one could assume that the H atom can be more easily transferred between O5 and O41 (due to the increased thermal motion), whereas the answer to "why at low temperature **A'** is favoured over **B'** form" remains open (the authors have performed the RT/LT data collection and structure refinement for **3** twice – on different crystals – with consistent findings).

For both rotamers of tautomer **D** (structures **4** and **5**) the imine hydrogen atom is unambiguously determined from the difference Fourier maps of the RT and LT experiments.

In all of the studied crystal structures the molecule shows similar geometrical characteristics of the pyrazolone and aromatic rings. The values of the torsion angles C4-C41-C42-C47, C3-C4-C41-O41 and C16-C11-N1-C5 (Table 2) express the variations of the molecule geometry, related to the rotation of the aromatic rings with respect to the pyrazolone. The presence of a strong intramolecular O-H…O hydrogen bond reduces the rotational flexibility around C4-C41 bond in tautomers **A'** and **B'** (structures **1**, **2** and **3**), while there are no such limitations in **D** tautomer (Schemes 1, 2). Thus we can hypothesize that the forms possessing intramolecular hydrogen bond (**A'** and **B'**) would be energetically more stable than the other possible rotamers of **A** and **B** forms, especially in gas phase or solution where intermolecular hydrogen bonds are hampered to some extent by the solvent. This is also supported by DFT calculations which show that the energetic minima of tautomers **A** and **B** are the rotamers exhibiting O-H…O intramolecular hydrogen bond (e.g. **A'** and **B'** forms, Table S2). This is expressed by the value of C3-C4-C41-O41 angle which is about 180°; 167.52(19)° in **1**; 168.2(3)° in **2** and 173.2(7)° in **3**. In structures **4** and **5** the proton is associated with N2. The N2 nearby atoms are carbons from the phenyl and methyl groups, which are not suitable acceptors for the formation of intramolecular hydrogen bond. Thus the

Table 2 Torsion angles expressing the variations of the molecule geometry in **1**-**5**.

Structure	Torsion angles in °		
	C4-C41-C42-C47	C3-C4-C41-O41	C16-C11-N1-C5
1	146.83(18)	167.52(19)	-9.6(3)
2	140.9(2)	168.1(2)	-12.4(3)
3	38.3(8)	-173.2(6)	-31.6(8)
4	-162.35(18)	31.0(3)	-25.1(3)
5	-160.97(18)	-142.7(2)	-48.6(3)

molecular packing in both structure **4** and **5** is stabilized by a N2-H2…O5 intermolecular hydrogen bond connecting molecules in both structures to chains running along ***c*** crystallographic direction. This intermolecular hydrogen bond is responsible for the higher melting points of **4** and **5**. A weak intramolecular hydrogen bond C16-H16…O5 is observed in structures **1**, **2**, **3** and **4**. In **5** although H16…O5 distance is 2.633 Å the angle *D*-H…*A* (e.g. C16-H16-O5) of 104.7° is too "acute" and not suited for such an interaction. Clearly the molecular geometry in structures **4** and **5** is governed by the C=O groups rotation around C4-C41 bond. In both structures the angle between the pyrazolone and phenyl ring's mean planes is 27.85° and 43.68° for 4 and **5** respectively. In structure **5** the deviation from planarity is more distinct, the conjugation less pronounced and thus the formation of the intramolecular C16-H16-O5 contact prevented (Table S2). For comparison, the pyrazolone and phenyl rings remain in almost one plane in **1** and **2** with angle between the ring's mean planes of 7.34(1)° and 9.55(1)° respectively, while in **3** this angle is 33.72(2)°.

The molecular geometry and three-dimensional packing in **1**-**5** are additionally stabilized by several short contacts (of CH…O, CH_3…π and π…π types, Figures S4-S8).

All of the above described angle's values apply for the structural data obtained from the RT experiment. The LT conditions cause shrinkage of the unit cell parameters in all of the studied structures. This contraction is realized (at a molecular level) by concurrent slight deformations of the molecules and reductions of the intermolecular bonds (Table S3).

A solid state NMR study was carried out to support the results from single crystal X-ray diffraction. The ^{13}C and ^{15}N spectra of three individual polymorphs (**1**, **4** and **5**) and two mixtures (**1** + **2** and **2** + **3**) were recorded at RT. All samples showed identical powder XRD before grinding and before and after NMR analyses indicating that no phase transitions occurred during the sample preparation and acquisition. As expected, the colourless crystals **4** and **5** gave clearly distinguishable spectra (Table S4). The carbon spectra of both polymorphs display different chemical shifts for almost all nuclei; even aromatic resonances show different patterns (Figures 2 and S9). The signals for N-2 were registered at 162.66 ppm and 167.50 ppm for **4** and **5**, respectively, which is compatible with sp^3 hybridized N-2 in both compounds.

The situation with the yellow polymorphs was initially more complicated as only **1** was grown as a single phase, while **2** and **3** were isolated as crystal mixtures. Fortunately, further cystalization experiments from ethanol-water led to isolation also of **1**+**2** mixture and a **2**+**3** fraction containing less than 10 % **2** according to powder XRD (Figures 2 and S2), which gave possibility to differentiate the spectra of both compounds. The signals of **2** were assigned by comparison of the spectra of **1**+**2** mixture with those of pure form **1** (Figure S10a), while the spectra of individual **3** were obtained from its >90 % enriched fraction.

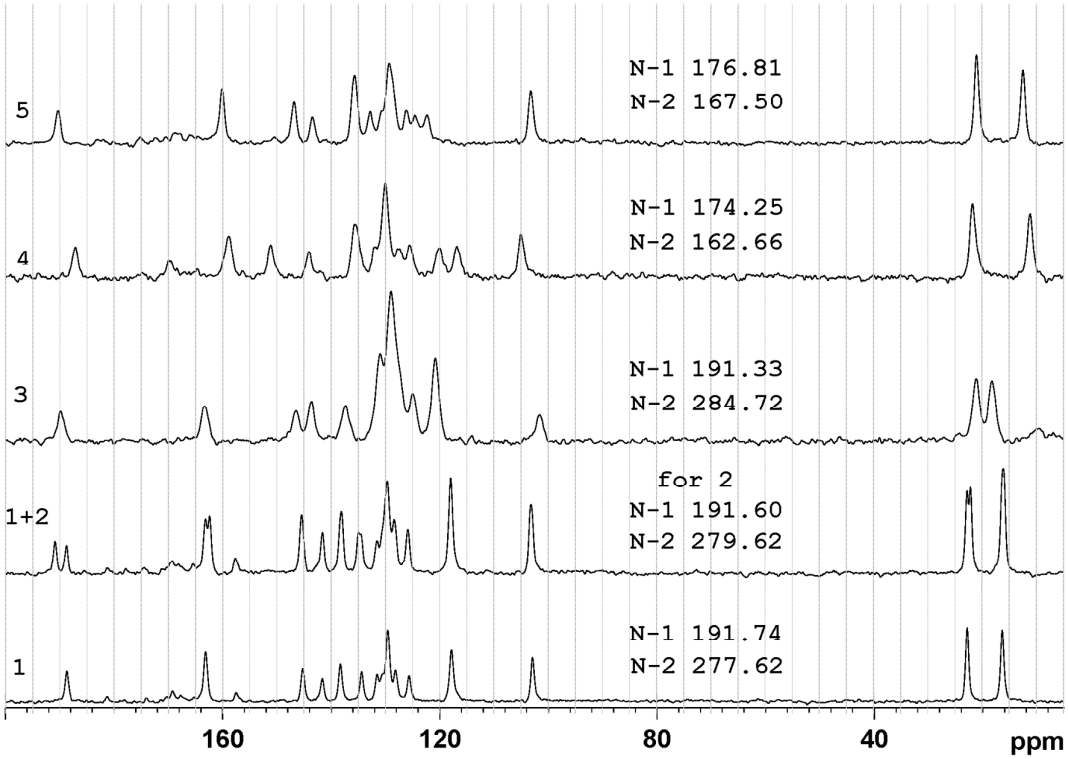

Figure 2 ^{13}C CPTOSS spectra of polymorphs **1**, **1**+**2** mixture, **3** (>90 %), **4**, and **5** with ^{15}N NMR resonances indicated.

The three yellow polymorphs possess different spectra, as illustrated on Figure 2 and Table S4. While the carbon resonances of **1** and **2** are quite similar, the biggest difference of 2.2 ppm was observed for the carbonyl group, the difference in the pattern of **3** is more significant. It should be noted, that the signals of the latter are broad most probably due to exchange (phase transitions). The latter is in full agreement with the crystallographic data.

The conformational preferences in solution were studied by NMR in several solvents (Figures S11-S13). The spectra were recorded in deuterated analogues of the solvents used for crystal growth - chloroform, methanol, acetone, and methanol/acetone 5:1 mixture. Several characteristic features are observed. NOESY spectra show clear cross peaks between pyrazolone methyl protons and ortho-tolyl protons in all solvent systems (Figure S13), indicating possible presence of forms **1**, **2**, **3**, and **4**. The pyrazolone methyl proton signals move downfield in methanol and methanol-acetone mixture in respect to chloroform and acetone (Table S5, Figures 3 and S11), 2.234 and 2.201 vs 2.146 and 2.107, respectively. On the contrary, the corresponding methyl ^{13}C NMR shifts move upfield in the methanol containing solutions and the signals are apparently broadened, indicating exchange with one or

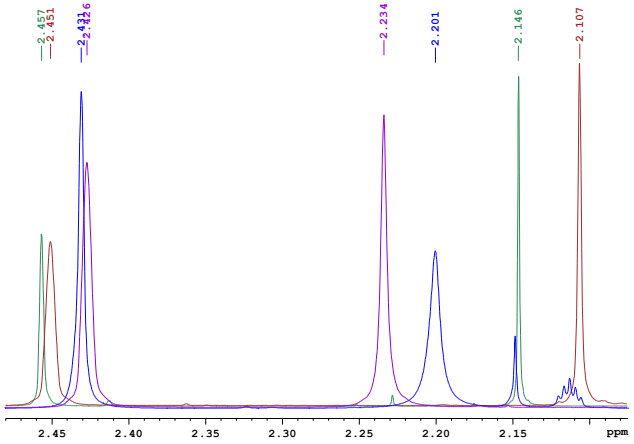

Figure 3 Methyl protons chemical shifts in: $CDCl_3$ (green), CD_3COCD_3 (brown), CD_3OD:CD_3COCD_3 5:1 (blue), CD_3OD (violet).

both NH forms. The latter is supported by the observed solid state chemical shifts. Additionally, small systematic differences of the pyrazolone ring carbon shifts (C-3, C-5, CH-2,6Ph) corroborate change of its electronic structure on solvent change. The fact that all crystal phases, yellow polymorphs **1**, **2**

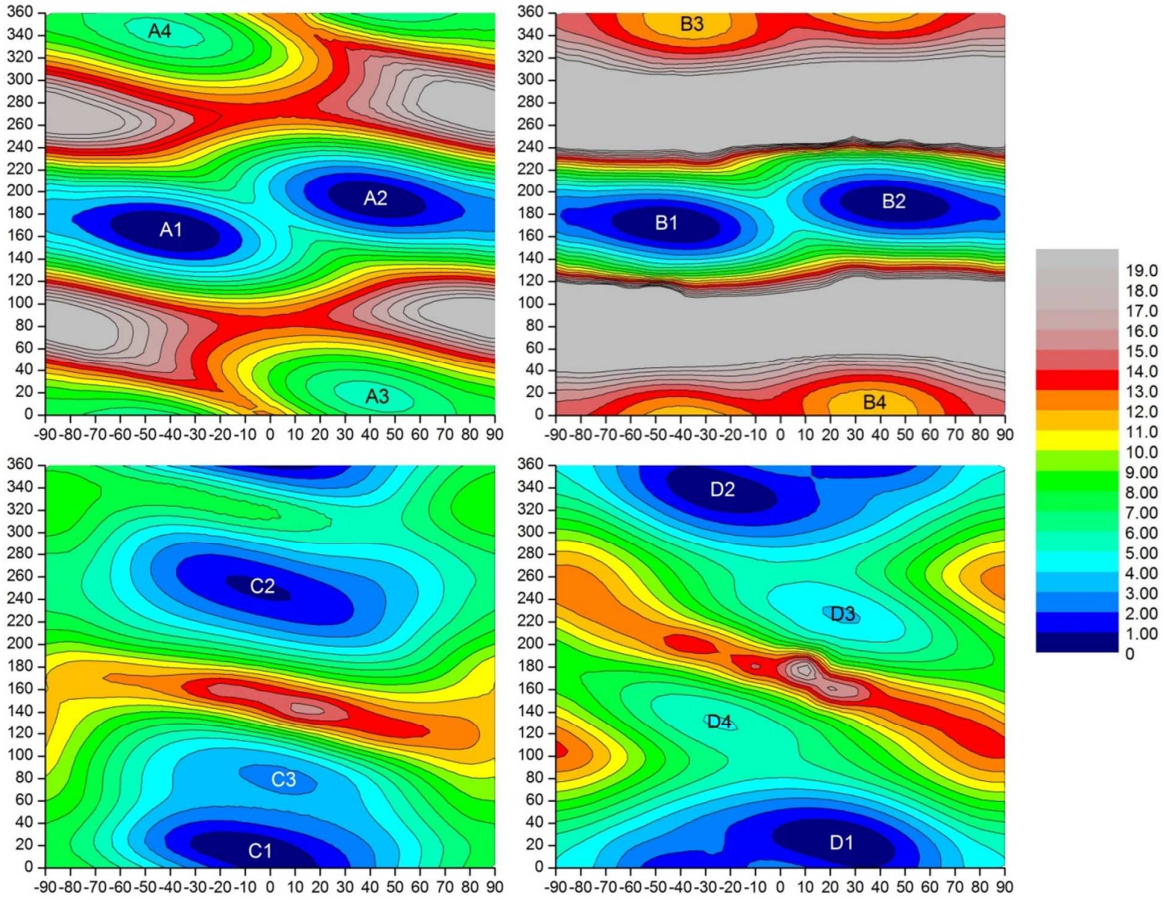

Figure 4 Energy as a function of variation of C4-C41-C42-C47 (X-axis) and C3-C4-C41-O41 (Y-axis) in the corresponding tautomers: **A** (top, left), **B** (top, right), **C** (bottom, left) and **D** (bottom, right). In each picture relative energy (in kcal/mol units) in respect of the most stable isomer of the corresponding tautomer is presented. The overall energy difference is shown in Table 2.

Table 4 Relative stability and major structural parameters of tautomers and isomers in gas phase (M06-2X/TZVP).

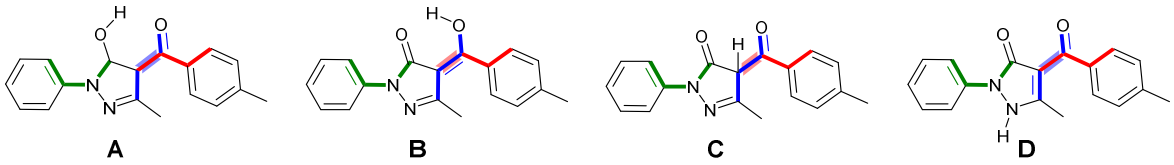

Structure	Dipole moment [D]	ΔE [kcal/mol]	ΔE+ZPE [kcal/mol]	ΔG [kcal/mol]	angle C4-C41-C42-C47	angle C3-C4-C41-O41	angle C16-C11-N1-C5
A1	2.61	0.00	0.00	0.00	-40.9	164.5	-26.3
A2	2.62	0.21	0.12	-0.26	41.7	-166.9	-22.7
B1	5.14	1.75	1.35	0.88	-44.1	170.1	-6.8
B2	5.14	1.75	1.35	0.88	44.1	-170.1	6.9
A3	4.73	5.44	5.08	4.63	41.1	16.7	-32.6
A4	4.84	5.46	5.20	4.90	-41.9	-17.7	-32.9
C1	3.59	9.01	8.17	7.02	-7.9	14.0	6.2
C2	3.78	9.85	8.96	7.62	-5.9	-109.5	-1.6
D1	4.12	10.34	9.87	9.43	24.0	22.4	-42.3
D2	3.78	10.51	9.92	8.98	-25.3	-21.8	-41.5
C3	6.35	11.74	10.91	9.54	4.3	81.7	10.7
B3	3.84	12.84	12.57	12.24	-36.5	-7.0	-12.7
B4	3.84	12.84	12.57	12.24	36.5	7.0	12.5
D3	7.60	14.21	13.58	11.35	24.2	-133.4	-37.8
D4	7.89	15.25	14.57	13.56	-24.2	130.2	-40.0

and **3** and colourless forms **4** and **5**, were grown from yellow solutions, indicates that small amounts of all forms could be present in solution. These results are in agreement with Holzer *et al.*[10] that in non-polar solvents like $CDCl_3$ and acetone the chelated hydroxy-form predominates, while in methanol containing solutions forms like **4** or **5** get more populated most probably because of their ability to stabilize the NH form via H bonding.

Potential energy surfaces of the tautomers as a function of C4-C41-C42-C47 and C3-C4-C41-O41 dihedral angles are shown in Figure 4. Some of the structural data and energies of the most stable isomers are collected in Table 4.

As seen from these data tautomers **A**, **B** and **D** exist as isomeric pairs which can easily interconvert. These are **A1**/**A2** and **B1**/**B2** as hydrogen bonded structures and **A3**/**A4** and **B3**/**B4** where the intramolecular hydrogen bonding is broken. The barriers between **A1** and **A2** (resp. **B1** and **B2**) are negligible. Similar is the situation with **A3**/**A4**, but the transfer from **A1**/**A2** to **A3**/**A4** needs substantial energy to occur. The transfer from **B1**/**B2** to **B3**/**B4** exceeds 20 kcal/mol, which is expected, taking into account that rotation around double bond is energetically demanding. The transfer from **A1** to **B1** proceeds with a barrier of 3.2 kcal/mol in gas phase and 3.3 kcal/mol in MeOH.

The situation in **D** is different – easy conversion is possible from **D1** to **D2**, but also each of them can isomerize to the corresponding less stable **D4** and **D3**, resp. Only in this case the direct transfer from **D3** to **D4** seems energetically unflavoured at least in gas phase.

The crystal structures and predicted by DFT geometries are in an excellent agreement. As seen on Figure 5, root mean square deviation (rmsd) values in the range of 0.1171-0.327 Å were obtained.

Considering the dipole moments, collected in Table 4, the effect of the solvent as a medium could not be sufficient to explain coexistence of **A** and **D** tautomers in solution. As already mentioned, the latter was not detected by NMR, which does not discard its existence. The corresponding calculations in methanol (as medium modelled by PCM; Table S6) show that **D** tautomers are strongly stabilized, but not sufficiently to be assumed to exist in solution. Most probably the stabilization of **D** could be a result of proton acceptor (directed towards N-H) and/or proton donor (two free carbonyl groups) action of the solvents.

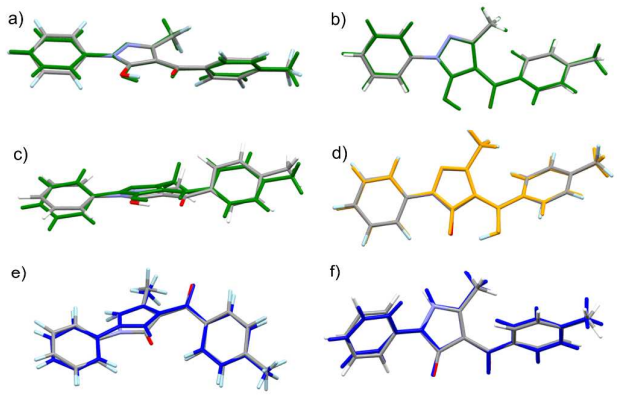

Figure 5 Overlay of: a) **1** (in green) and **A1**, rmsd 0.1814 Å; b) **2** (in green) and **A1**, rmsd 0.1262 Å; c) **3** (in green) and **A2**, rmsd 0.327 Å; d) **3** (in orange) and **B1**, rmsd 0.1171 Å; e) **4** (blue) and **D1**, rmsd 0.2395 Å; f) **5** (blue) and **D3**, rmsd 0.1893 Å.

Experimental

All reagents were purchased from Merck and Fluka and were used without any further purification. Fluka silica gel/TLC-cards 60778 with fluorescent indicator 254 nm were used for TLC chromatography. The melting points were determined in capillary tubes on SRS MPA100 OptiMelt (Sunnyvale, CA, USA) automated melting point system. The NMR spectra were recorded on standard bore Bruker AVII+ 600 and HD 500 spectrometers (Rheinstetten, Germany) at RT. The chemical shifts were referenced in ppm in δ-values against tetramethylsilane (TMS) as an internal standard for the liquid state. The external standard α-glycine (43.5 ppm for ^{13}C and 33.4 ppm for ^{15}N) was used for the solid state. Unambiguous assignment in solution was done by applying standard 2D NMR techniques that was used for comparison and discrimination of the signals in the solid state. The spectra were recorded as $3x10^{-2}$ M solutions in order to avoid intermolecular interactions (for reliable shifts and NOE enhancements). The spectra were processed with Topspin 2.1 program.

Solid state ^{13}C and ^{15}N NMR spectra were recorded on a 4 mm double resonance CPMAS probe-head. The sample was ground softly with a mortar and pestle and then packed tightly in a 4-mm zirconium oxide rotor. Samples were spun at 6.0 kHz for all experiments. Typical radio-frequency (RF) field strengths were 30-65 kHz for ^{13}C and ^{15}N. The Hartmann–Hahn polarization transfer was optimized to a contact time of 2 ms for ^{13}C and 4 ms for ^{15}N with a linear ramp starting at 50%. ^{13}C NMR spectra were obtained using a combination of CP/MAS and total sideband suppression (TOSS) methods (CP/MAS/TOSS) with SPINAL64 proton decoupling. Non Quaternary Suppression (NQS) technique via 60 μs dipolar dephasing was applied to distinguish unambiguously the quaternary carbons. 512 transients for ^{13}C and 4096 for ^{15}N were typically accumulated with 5 and 4 s relaxation delay.

Single-crystal X-ray diffraction data were collected at room (RT) and low temperature (LT) conditions using the same single crystal for each of the studied samples. The RT (290K) and LT (150 K) data collections were performed by ω-scan technique, on an Agilent Diffraction SuperNova Dual four-circle diffractometer equipped with Atlas CCD detector using mirror-monochromatized MoKα radiation from micro-focus source (λ = 0.7107 Å). During the LT data collection the samples were kept at 150 K with an Oxford Instruments Cobra device and a nitrogen atmosphere. The determination of cell parameters, data reduction and absorption corrections were carried out using the CrysAlis Pro program package.[16] The structures were solved by direct methods (SHELXS-97)[17] and refined by full-matrix least-square procedures on F^2 (SHELXL-97).[17] Crystallographic data were deposited with Cambridge Crystallographic Data Centre: Deposition numbers CCDC 1406726-1406735. Copies of the data can be obtained free of charge on application to CCDC, 12 Union Road, Cambridge CB2 1EZ, UK (fax: (44) 1223336-033; e-mail: deposit@ccdc.cam.ac.uk).

Powder – Xray diffraction experiments were carried on a diffractometer D2 PHASER AXS - Bruker, equipped with Bragg-Brentano horizontal goniometer (2θ) and scintillation counter using Ni-filtred CuKα radiation (λ = 1.5406 Å). The data were recorded at room temperature in the interval of 4o>2θ>50o with a step at of 0.04 2θ and scanning time 2s. The experimental data are presented on Figure S2.

Quantum-chemical calculations were performed by using the Gaussian 09 program suite[18] applying M06-2X fitted hybrid meta-GGA functional[19] with TZVP basis set.[20] It is worth mentioning that this method has been recently demonstrated as very suitable for describing tautomeric behaviour in azonaphthols and related Schiff bases[21] as well as for prediction of the absorption spectra of organic dyes.[22,23]

The tautomeric forms were optimized without restrictions in gas phase under tight optimization conditions by using ultrafine grid in the computation of the two-electron integrals and their derivatives. The optimized structures were then characterized as true minima by vibrational frequency calculations.

The potential energy surface of each of the four tautomers was investigated as a function of angles C4-C41-C42-C47 and C3-C4-C41-O41, which were changed with step of 10° and optimization of the remaining part of the molecule was performed at normal optimization conditions.

In all cases the solvent medium was described by using the PCM model, namely IEFPCM,[24] as implemented in Gaussian 09. The transition states were calculated using the STQN method for locating transition structures[25] as implemented in Gaussian 09.

Conclusions

The conformational behaviour of 3-methyl-4-(4-methylbenzoyl)-1-phenyl-pyrazol-5-one was studied by single crystal and powder X-ray diffraction, NMR spectroscopy in solution and in solid state, and DFT calculations in gas phase. The combined analysis leads to the following conclusions:

1. In solution the molecular conformation is governed by the establishment of internal O-H…O hydrogen bond (yellow coloration of the solutions).
2. The observed **D** to **A**/**B** form interconversion of the molecular geometries in solution is consistent with DFT calculation revealing smaller energy barriers between **A**, **B** and **D** forms.
3. Although NMR signals of the keto form could not be detected in solution the fact that single crystals grown form those yellow coloured solutions, displaying a keto molecular geometry (**4**, **5**), show that the keto form is also present.
4. While in solution one can clearly state the prevalence of the importance of the internal hydrogen bond, the 3D packing of the molecules in the crystal structures is additionally determined by the type of the rotamer.
5. The structural features of rotamers are dependent on the weak interactions stabilizing the crystal structure (or *vice versa*).
6. The solvent effect on the tautomerism could not be satisfactorily explained neither by DFT (PCM calculations) nor by NMR experiments in different solvent media.

Five different crystal phases of 3-methyl-4-(4-methylbenzoyl)-1-phenyl-pyrazol-5-one were grown and characterized by single crystal XRD and solid state NMR as three desmotrops, two of them as two different conformational polymorphs. To the best of our knowledge, that is the first record in the literature on the isolation of more than two desmotrops.

Acknowledgements

The financial support by The Bulgarian Science Fund, projects UNA-17/2005, DRNF-02-13/2009, RNF-01/0110, and DRNF-02/01, and by EU, project FP7-REGPOT-2011-1/286205 “Beyond Everest”, is gratefully acknowledged.

Notes and references

1 a) J. Bernstein, *Polymorphism in Molecular Crystals*; Clarendon Press: Oxford, 2002; b) A. Nangia, *Acc. Chem. Res.*, 2008, **41**, 595; c) J.-P. Brog, C.-L. Chanez, A. Crochet and K. M. Fromm, *RSC Adv.*, 2013, **3**, 16905; d) A. J. Cruz-Cabeza and J. Bernstein, *Chem. Rev.*, 2014, **114**, 2170; e) P. Naumov and S. C. Sahoo, in *Tautomerism. Methods and Theories*, ed. L. Antonov, Wiley-VCH: Weinheim, Germany, 2014, chapter 8, pp. 197-212.
2 a) S. R. Byrn, R. R. Pfeiffer and J. G. Stowell, *Solid State Chemistry of Drugs*, SSCI, Inc.: West Lafayette, IN, 1999; b) D. A. Snider, W. Addicks and W. Owens, *Adv. Drug Deliv. Rev.*, 2004, **56**, 391; c) R. Hilfiker, *Polymorphism in the Pharmaceutical Industry*, Wiley-VCH Verlag GmbH & Co. KgaA: Weinheim, Germany, 2006; d) H. G. Brittain, *Polymorphism in Pharmaceutical Solids*, 2nd ed., Informa Healthcare USA, Inc.: New York, 2009, Vol. 192.
3 J. Elguero, *Cryst. Growth Des.,* 2011, **11**, 4731.
4 a) Y. A. Zolotov and N. M. Kuzmin, *Extraction of Metals by Acylpyrazolones*, Nauka: Moscow, Russia, 1977; b) C. Pettinari, F. Marchetti and A. Drozdov in *Comprehensive Coordination Chemistry II*, Elsevier, 2003, Vol. 1, chapter 1.6, pp. 97-115; c) F. Marchetti, C. Pettinari and R. Pettinari, *Coord. Chem. Rev.*, 2005, **249,** 2909; d) F. Marchetti, R. Pettinari and C. Pettinari, *Coord. Chem. Rev.*,2015, **303**, 1.
5 B. S. Jensen, *Acta Chem. Scand.*, 1959, **13**, 1890.
6 F. Stoltz, *J. Prakt. Chem.*, 1897, **55**, 145.
7 B. S. Jensen, *Acta Chem. Scand.*, 1959, **13**, 1668.
8 A**.** Michaelis and F. Engelhardt, *Ber. Dtsch. Chem. Ges.*, 1908, **41**, 2668.
9 W. Holzer, B. Plagens and K. Lorenz, *Heterocycles*, 1997, **45**, 309.
10 W. Holzer, K. Mereiter and B. Plagens, *Heterocycles*, 1999, **50**, 799.
11 W. Holzer, R. M. Claramunt, C. López, I. Alkorta and J. Elguero, *Solid State Nucl. Magn. Res.*, 2008, **34**, 68.
12 CCDC Number 664612; P. N. Remya, C. H. Suresh and M. L. P. Reddy, *Polyhedron*, 2007, **26**, 5016.
13 L. N. Kurkovskaya, N. N. Shapet'ko, A. S. Vitvitskaya and I. Y. Kvitko, *Zh. Org. Khimii*, 1977, **13**, 1750.
14 V. B. Kurteva and M. A. Petrova, *J. Chem. Educ.*, 2015, **92**, 382.
15 R. Meera and M. L. P. Reddy, *Solvent Extr. Ion Exch.*, 2004, **22**, 761.
16 CrysAlis PRO, Agilent Technologies, UK Ltd, Yarnton, England, 2011.
17 G. M. Sheldrick, *Acta Cryst. A,* 2008, **64**, 112.
18 M. Frisch, G. Trucks, H. Schlegel, G. Scuseria, M. Robb, J. Cheeseman, G. Scalmani, V. Barone, B. Mennucci, G. Petersson, H. Nakatsuji, M. Caricato, X. Li, H. Hratchian, A. Izmaylov, J. Bloino, G. Zheng, J. Sonnenberg, M. Hada, M. Ehara, K. Toyota, R. Fukuda, J. Hasegawa, M. Ishida, T. Nakajima, Y. Honda, O. Kitao, H. Nakai, T. Vreven, J. Montgomery, Jr., J. Peralta, F. Ogliaro, M. Bearpark, J. Heyd, E. Brothers, K. Kudin, V. Staroverov, R. Kobayashi, J. Normand, K. Raghavachari, A. Rendell, J. Burant, S. Iyengar, J. Tomasi, M. Cossi, N. Rega, J. M. Millam, M. Klene, J. Knox, J. Cross, V. Bakken, C. Adamo, J. Jaramillo, R. Gomperts, R. Stratmann, O. Yazyev, A. Austin, R. Cammi, C. Pomelli, J. Ochterski, R. Martin, K. Morokuma, V. Zakrzewski, G. Voth, P. Salvador, J. Dannenberg, S. Dapprich, A. Daniels, O. Farkas, J. Foresman, J. Ortiz, J. Cioslowski, and D. Fox, Gaussian 09, Revision A.02, Gaussian, Inc., Wallingford CT, 2009.
19 a) Y. Zhao and D. G. Truhlar, *Theor. Chem. Acc.,* 2008, **120**, 215; b) Y. Zhao and D. G. Truhlar, *Acc. Chem. Res.*, 2008, **41**, 157.
20 F. Weigend and R. Ahlrichs, *Phys. Chem. Chem. Phys*., 2005, **7**, 3297.
21 S. Kawauchi and L. Antonov, *J. Phys. Org. Chem.*, 2013, **26**, 643.
22 See for details: A. Laurent, C. Adamo and D. Jacquemin, *Phys. Chem. Chem. Phys.*, 2014, **16**, 14334.
23 a) L. Antonov, V. Deneva, S. Simeonov, V. Kurteva, A. Crochet, K. Fromm, M. B. Shivachev, R. Nikolova, M. Savarese and C. Adamo, *ChemPhysChem*, 2015, **16**, 649; b) S. Kawauchi, L. Antonov and Y. Okuno, *Bulg. Chem. Commun*., 2014, **46 Special Issue A**, 228.
24 J. Tomasi, B. Mennucci and R. Cammi, *Chem. Rev.*, 2005, **105**, 2999.
25 C. Peng, P. Y. Ayala, H. B. Schlegel and M. J. Frisch, *J. Comp. Chem.*, 1996, **17**, 49.